

SOME INTERESTING CONCLUSIONS FROM A STUDY OF Q-ATTENUATION

SUDHIR JAIN¹

ABSTRACT

A review of available literature and considerable modelling and experimental work show that Q can be estimated from seismic reflection recordings in three different ways which provide generally consistent values. Estimated Q-values can be used to predict the attainable resolution of field data and to correct for dispersion, which is the main cause of sonic-seismic misties. It appears that the deconvolution normally applied in the early stages of processing compensates for distortion and delays caused by attenuation within the seismic frequency band.

INTRODUCTION

Attenuation of seismic waves with travelled distance has been studied theoretically in both field and laboratory during the last thirty years. Knopoff and McDonald (1958), McDonal *et al.* (1958), O'Brien (1961), Futterman (1962), Trorey (1962), Gardner *et al.* (1964), Wuenchel (1965), Bremaecker *et al.* (1966), Strick (1967, 1970, 1971), Ganley and Kanasewich (1980) and Winkler (1986) among others have published excellent works on various aspects of attenuation.

As the elastic waves travel deeper, they lose energy as it is partially converted into heat. This loss is frequency dependent — higher frequencies are absorbed more rapidly than lower frequencies, such that the highest frequency recovered on most seismic data is about 80 Hz. A combination of gain adjustment and deconvolution compensates for this loss to some extent, but the energy below a certain level cannot be recovered. This causes reduction in resolution as well as a limitation to the penetration of seismic energy. Moreover, absorption appears to vary with the lithology of the medium. The unconsolidated near surface absorbs more energy than the underlying compact rocks. The changes in this zone may be the source of amplitude variations on seismic records, which may be confused with lithologic changes in the zone of exploration interest. In extreme cases, most of the energy may be absorbed in the first few hundred metres of the subsurface.

It is, therefore, important to study the absorption and determine the ways in which it can manifest itself on seismic data. A detailed study of a simple absorption law by Averbukh (1963) was conducted by Crowe and Alhilali (1974) who related absorption to dispersion — variation of velocity with frequency — and showed that practical values of absorption coefficients can cause a change in velocity of 2% to 4% between frequencies of sonic log source and those of seismic waves on field records. Gretener (1961) had noted a systematic discrepancy of up to 3% between sonic log and check shot times, and ascribed it to anisotropy and dispersion. Strick (1971) showed that this discrepancy can be fully explained by his power-law attenuation model as the pedestal effect. Stewart *et al.* (1984) observed an average discrepancy of 2.0 ms/1000 ft between integrated sonic times and vertical seismic profiles, and showed that most of this discrepancy can be due to dispersion predictable from the constant Q model. Winkler (1986) states that the velocity dispersion is of an appropriate magnitude to explain differences between seismic and sonic log frequency. In this paper, we discuss some implications of absorption related to the spectrum of field data and show that absorption coefficients can be determined from seismic data, alone or in conjunction with sonic logs, and used to adjust sonic log velocities. We also show by practical examples that the change in velocity with frequency as computed from realistic Q-values fully explains the time mistie between the sonic log and seismic data. Sonic log velocities after adjustment for dispersion with estimated Q-values provide synthetics that match seismic data throughout their lengths and minimize confusion in polarity on synthetics from unadjusted velocities.

DESCRIPTION OF THE PROBLEM

The attenuation of a wavelet travelling in an inelastic medium takes two forms. First, it loses energy: generally, the higher the frequency the greater the loss. Second, it is to be expected that the phase component of the

¹Commonwealth Geophysical Development Company, Ltd., #1701, 505 - 3 Street S.W., Calgary, Alberta T2P 3E6.

The cooperation of my colleagues at Commonwealth Geophysical is acknowledged. The author benefitted from his many discussions with W.W. Soukoreff of Petro-Canada, D. Hargrave of Home Oil, and W.L. Kelsch of PanCanadian Petroleum.

wavelet suffers delay related to frequency. In other words, different frequency components travel with different velocities. Indeed, it is borne out by general experience that synthetic seismograms generated from sonic logs where frequencies are of the order of 20K Hz usually need to be stretched to match the seismic traces, *i.e.* have travelled with higher velocities. Gretener (1961) showed from his study of sonic logs and check shots in Alberta that the sonic logs are compressed 1 to 2.5 ms per 1000 ft. This indicates that the velocity for waves of frequencies used in sonic logs is 1% to 2.5% higher than for waves of seismic frequencies travelling at 10,000 ft/s. The attenuation and consequent dispersion has two implications in the interpretation of seismic reflection data. First, wavelets are expected to become distorted as they travel downward. Second, seismic traces match the synthetic seismograms for only short stretches, and problems are encountered in identifying markers and establishing polarities.

There is no consensus regarding the magnitude of phase distortion except that dispersion within seismic record frequencies is expected to be considerably less than one percent and, by itself, becomes less serious at greater depths because the spectrum becomes quite narrow. It is possible that the delay in the minimum phase wavelet caused by the loss of high frequencies is sufficient to account for this dispersion.

ATTENUATION EQUATION

Bremaecker *et al.* (1966) derived the relationship between amplitude A and distance d travelled by P-waves as:

$$A = md^{-2} \exp(-\pi f.d/V.Q) \quad (1)$$

where f is the frequency, V the velocity and Q the attenuation coefficient defined such that $2\pi/Q$ is the ratio of energy dissipated to that stored in a cycle. Higher Q means less absorption. For sedimentary rocks, Q generally ranges between 30 and 300 (McCarley, 1985). Unconsolidated material has lower Q . In shales and sandstones Q generally ranges from 50 to 150, and in carbonates from 100 to 300.

By substituting A_0 , amplitude very close to the source for md^{-2} , travel time $t = d/v$ and converting the equation to energy,

$$E = E_0 \exp(-2\pi ft/Q) \quad (2)$$

which is the same as the equation given by McCarley (1985) except that he writes it for period T instead of frequency f .

Equation (2) gives us a relationship between attenuation E/E_0 and t , Q and f . To understand the attenuation of seismic waves, it is helpful to hold either t or f constant and plot attenuation curves vs f or t for various values of Q .

Attenuation vs Frequency

Attenuation in db was plotted vs frequencies ranging from 10 to 110 Hz for travel times .25 to 2.5 s and for Q -values ranging from 30 (Pierre Shale) to 300 (massive carbonates). One example is shown in Figure 1 for $Q = 120$. Absorption is normalized to zero at the low-cut end and is plotted in db's up to -50 db. Note that the curves do not take into account either the instrument response or attenuations and compensations applied in data processing. Thus, these curves apply only the field recordings with instruments of flat response over the frequency band.

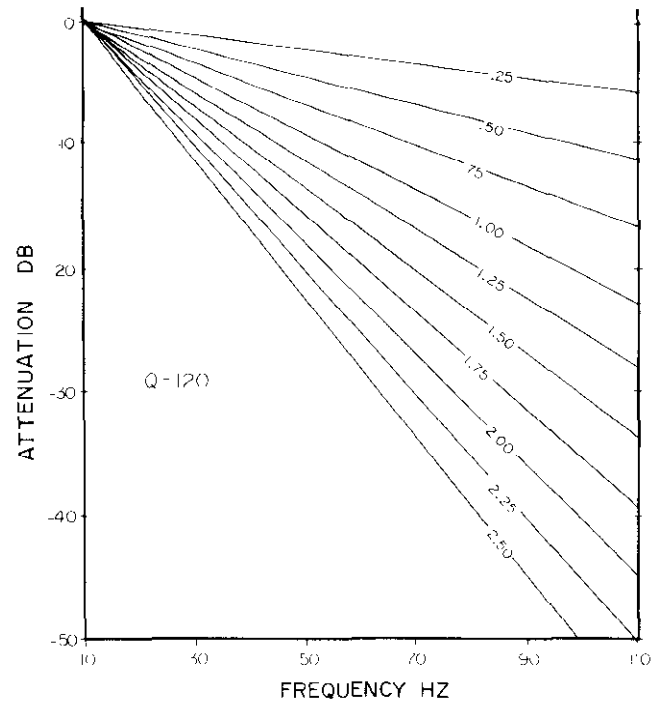


Fig. 1. Attenuation curve for $Q = 120$.

The threshold level where the energy at a particular frequency is irrecoverable depends on signal/noise ratio on the field records. In good record areas, -20 db is perhaps a reasonable threshold level. Therefore, we can define the frequency zone where transmission is above -20 db as the useful spectrum. The following conclusions can be derived from a set of absorption curves:

1. All curves linearly decline with increasing frequency irrespective of the Q -factor. Therefore, with increasing travel time frequency content of the data always shifts toward the lower end, the magnitude of the shift depending on the Q -factor and the travel time. The relative shift diminishes as the consolidation increases. As will be shown later, Wiener-Levinson deconvolution compensates for most of this high-frequency absorption and the delays it introduces.

2. In the presence of thick unconsolidated material ($Q = 30$ or less) the useful spectra are 10-100 Hz and 10-70 Hz when two-way times in this zone are .35 s and

.50 s, respectively. These times correspond to the thicknesses of 175 m and 250 m respectively when velocity is 1000 m/s. These parameters for the weathered zone are quite common in the Western Canada Basin, and it appears that the consolidation and thickness of the weathered zone are crucial parameters in defining the attainable resolution in a prospect.

3. For massive limestones and dolomites ($Q=300$) the useful spectrum extends beyond 100 Hz up to 2.5 s. Therefore, thick zones of carbonates do not alter the useful spectrum appreciably.

4. As the Q-factor increases, the rate of attenuation is diminished at all frequencies. In other words, high-frequency data indicate a higher Q-factor for the transmitting material, *i.e.* it is more consolidated.

5. Assuming an average Q value of 120, the useful spectrum is 10-100 Hz at .8 s (the time of Channel sands in southern and central Alberta), not accounting for weathering loss. Therefore, a direct correlation between a reflector and thin channel sands is improbable regardless of the type of source used in the survey, although improvements in current data are possible.

6. Assuming an average Q-value of 150, the useful spectrum is 10-100 Hz at 1.2 s (Slave Point marker). Therefore, thin porosity zones in carbonates will be observed on the seismic section only indirectly, even in the best recorded data. Again, improvements in existing data are possible.

Attenuation vs Time

Attenuation in db was plotted vs travel time up to three seconds for Q-values ranging from 50 to 290 and frequencies from 20 to 100 Hz. One example of these attenuation curves for a frequency of 40 Hz is shown in Figure 2. The figure shows that for a seismic wavelet whose dominant frequency is 40 Hz, the attenuation rate is 4.0 db/s for $Q=250$, 6.6 db/s for $Q=170$ (carbonates) and 11.6 db/s for $Q=50$ (lower end of the range for sandstones and shales). In other words, such a wavelet is not expected to be observed on field records below 2.0 s in Mesozoic and Cenozoic sections.

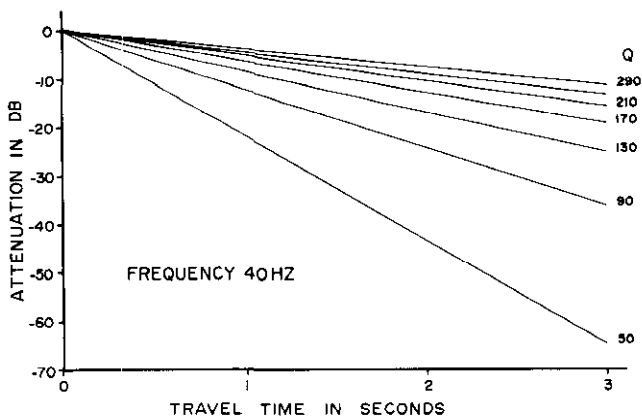


Fig. 2. Inelastic attenuation curves for the frequency of 40 Hz and various values of Q.

Deconvolution

Equation (2) gives us the means to compute power spectra for various values of Q and t and, therefore, the minimum or zero phase wavelets at any given time for any value of Q. The equation also allows the computation of Q from the power spectrum of the field traces, as will be discussed in a later section.

Figure 3 shows two sets of 12 traces each. Right twelve traces show minimum phase wavelets calculated from amplitude spectra according to Equation (2) for $Q=30, 50, 70, \dots, 250$. Cosine truncation such that spectra were reduced to half the calculated value at 70 Hz and to zero at 100 Hz was applied. A 10-Hz low-cut filter was also applied. Both sets have been corrected for spherical divergence. As would be expected, zero-phase wavelets show widening with increasing time and decreasing Q, but not time delays for the peaks. Minimum phase wavelets show the widening in the same manner as zero-phase wavelets, and also the delay which becomes quite pronounced at low Q and high travel times. Figures 4 and 5 show the deconvolution of these data by using the Wiener-Levinson algorithm for minimum-phase and zero-phase output, respectively. Both sets now show similar wavelet shapes for all Q-values as well as all travel times, except for the data below the slanted lines where distortion was excessive because of extreme attenuation. Note that the events peak at identical times for all Q-values, indicating that the relative time shifts noted on the minimum-phase synthetics for different Q have been corrected. The wavelets show a decline in amplitude with increasing travel time, which corresponds to the attenuation rates of approximately 3.8 db/s for $Q=250$, 11.0 db/s for $Q=170$ and 13 db/s for $Q=50$. These rates are very similar to those observed in Figure 2.

The example shows that, in all but extreme cases of attenuation, deconvolution normally applied to field data is adequate to stabilize the wavelet and compensate for time-delay within the *wavelet spectrum band*. The correction for frequency differences two orders of magnitude larger between sonic frequencies (50 Hz) and sonic logs (20K Hz) is a different problem, which will be discussed later in the paper.

DETERMINATION OF Q FROM FIELD RECORDS

An examination of Equation (2) shows that Q can be determined either from the slope of a power spectrum or from energy for a specific frequency f at two different times. Both methods assume that

1. The spectrum of the reflectivity index series is white.
2. The instrument response is flat in between frequencies being used.
3. The source signal is white.
4. The extraneous noise is minimal.

Figure 6 shows the spectra from four different windows for the reflectivity index series computed from a

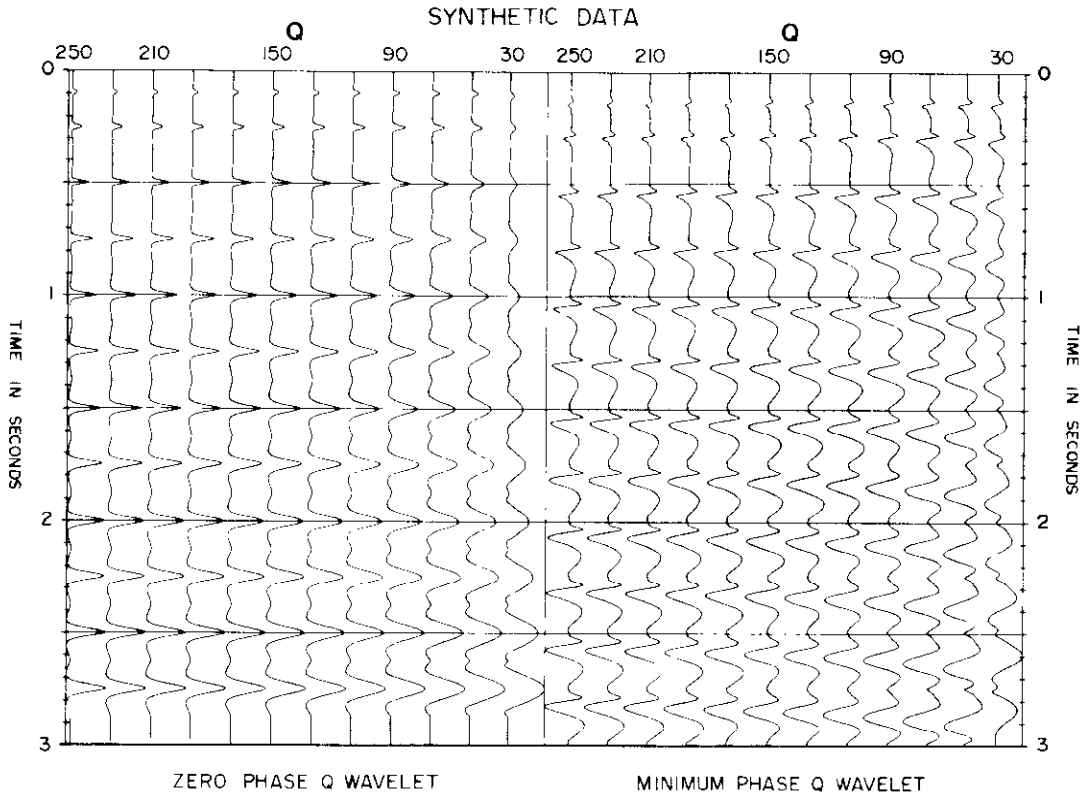


Fig. 3. Synthetic traces for Q ranging from 30 to 250. Right twelve traces assume minimum phase and left twelve zero phase.

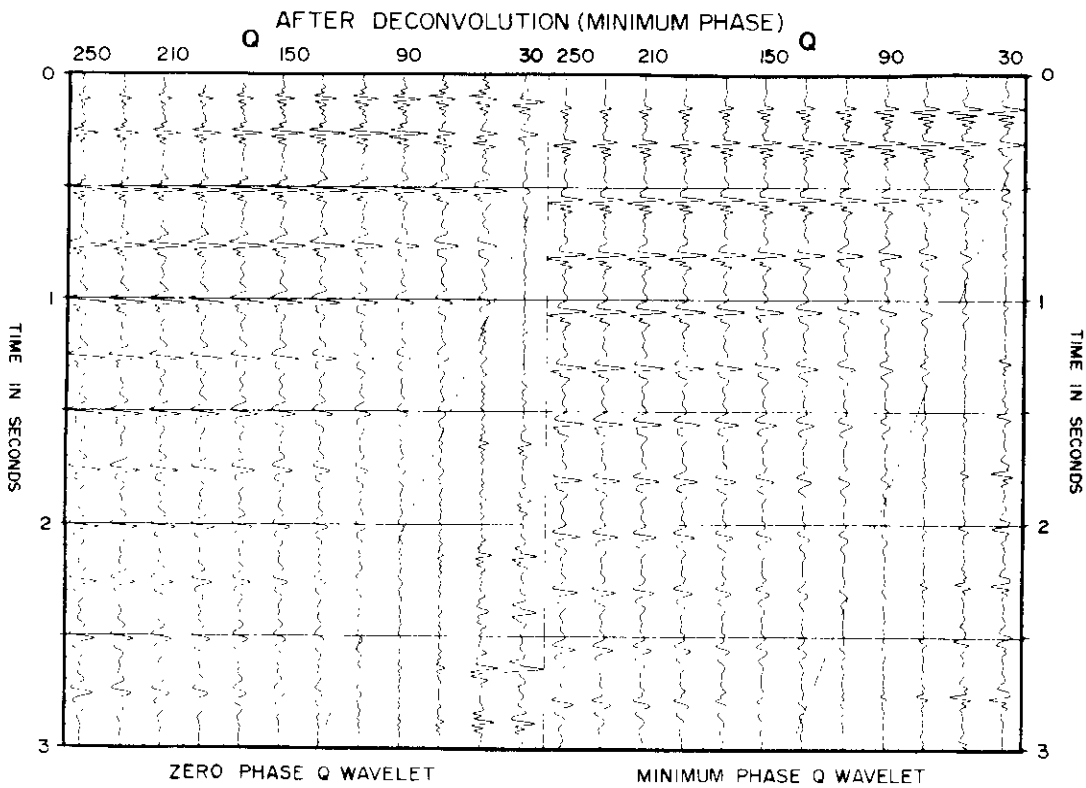


Fig. 4. Deconvolution of synthetic record in Figure 3 for minimum-phase output wavelet.

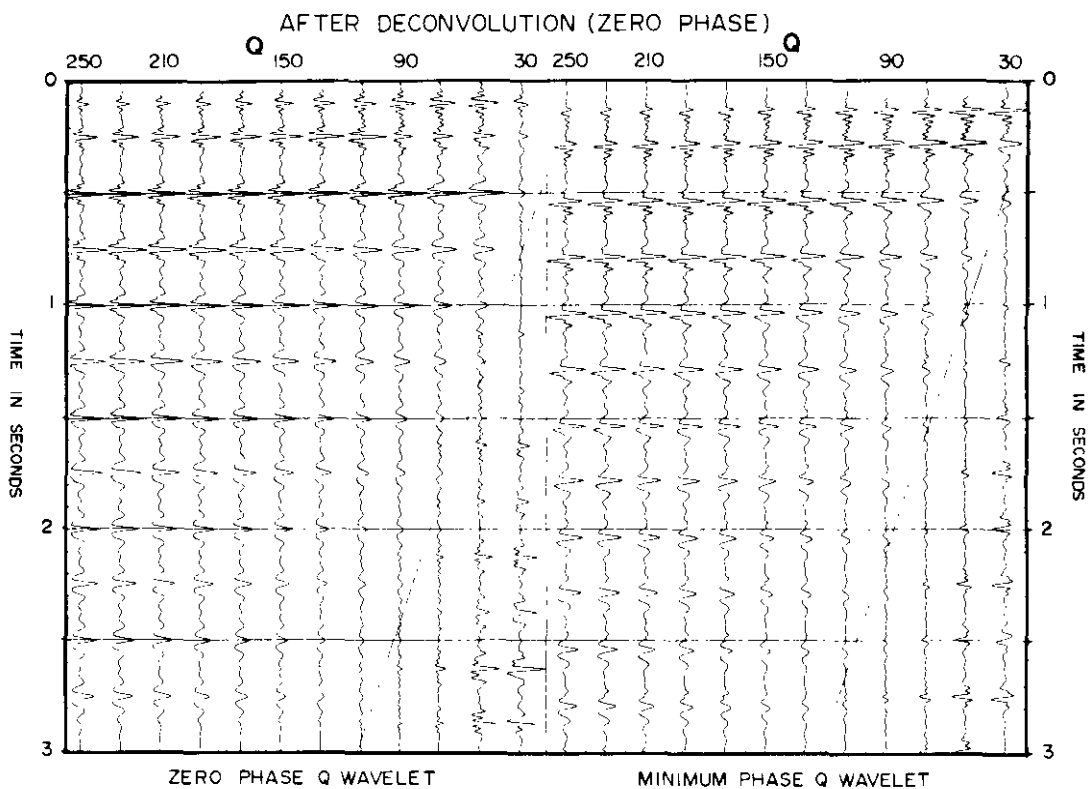


Fig. 5. Deconvolution of Figure 3 for zero-phase output wavelet.

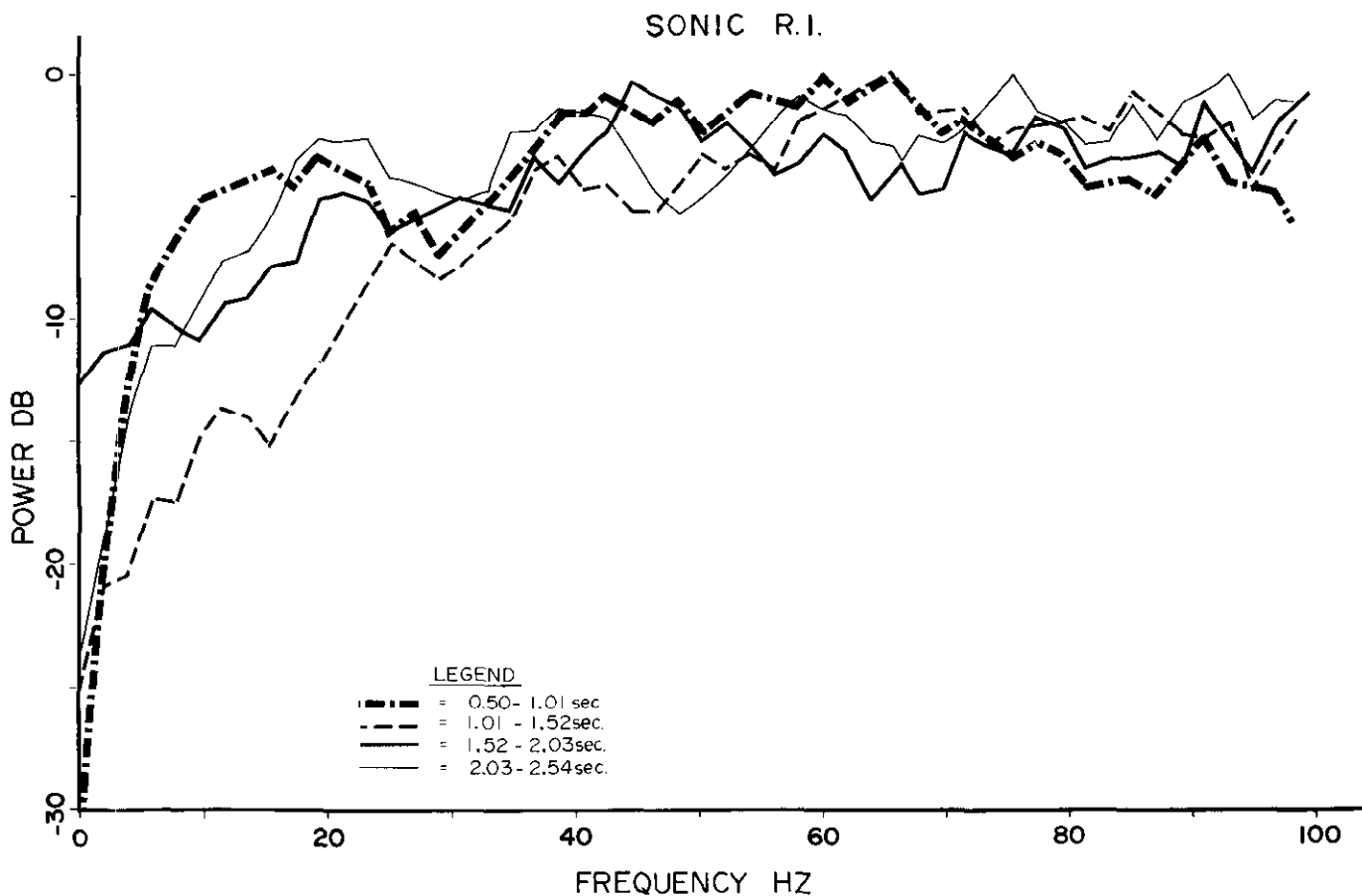


Fig. 6. Spectrum of reflectivity index series computed for a sonic log over four windows.

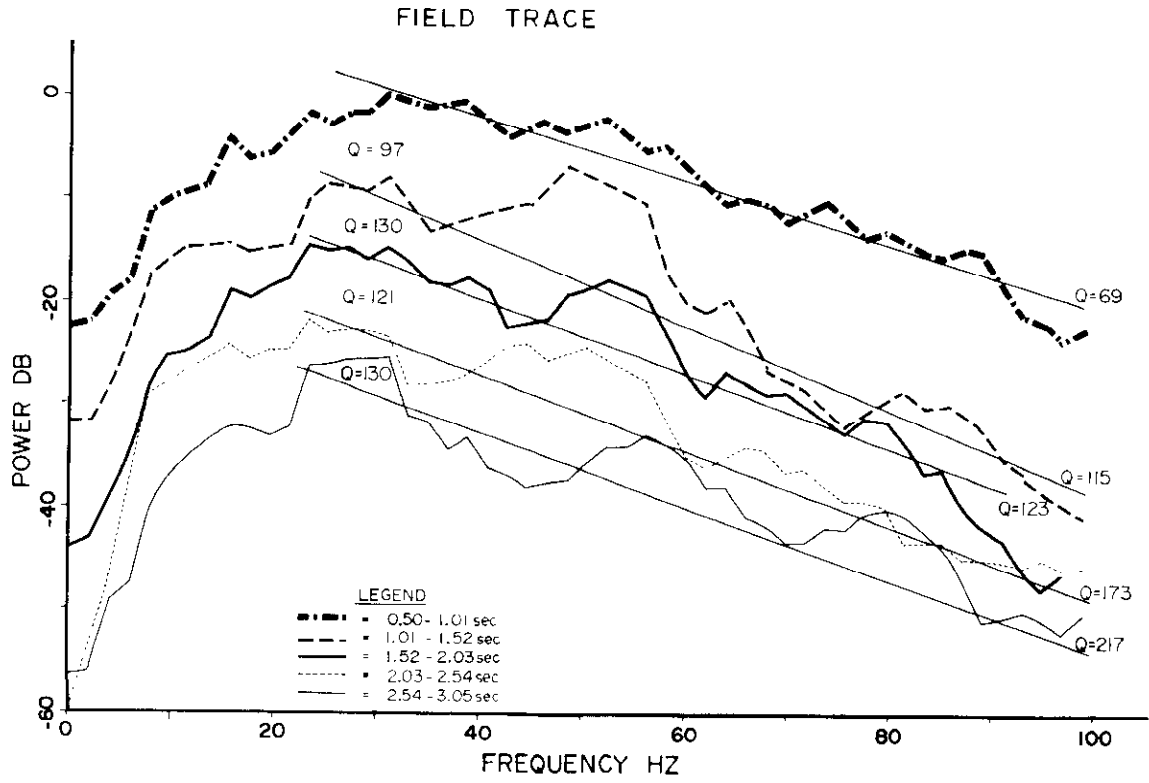


Fig. 7. Spectra over the field trace for five windows and computed Q-values.

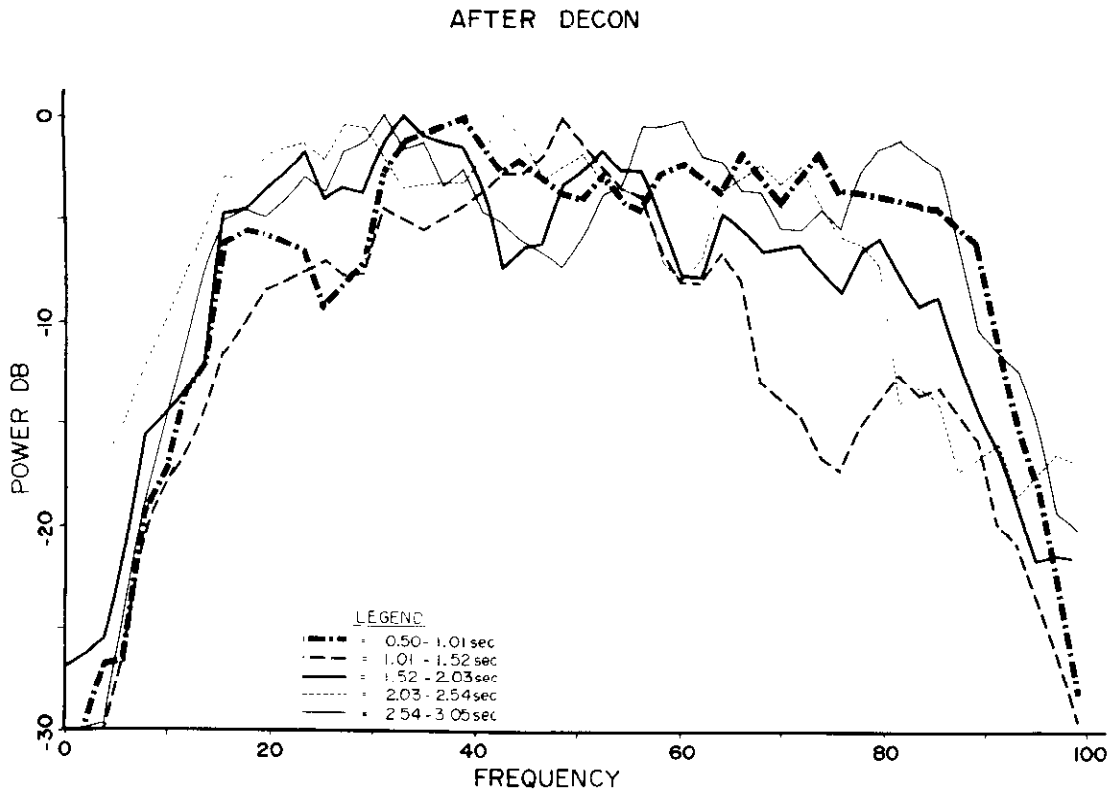


Fig. 8. Spectra over field trace after deconvolution.

deep sonic log from offshore Africa. The spectra generally show a positive slope between 10 and 60 Hz, which reduces the slope of the spectrum from the field trace and therefore increases the estimate of Q. The assumptions on source and instrument responses are generally valid, particularly after correction for instrument response. Extraneous noise is unpredictable and can be avoided only by selecting relatively noise-free traces.

Figure 7 shows five spectra from a field trace located very near the well used in Figure 6. Q-values estimated from the slope are given at the right end of each curve. Q-values estimated from frequencies around 30 Hz are shown in between the curves. Except for the deepest pair of windows, where the signal/noise ratio is low, there is a general correspondence in the two sets of values, although they are by no means identical.

For the sake of general interest, spectra for the same windows are shown after spiking deconvolution in Figure 8 and after stack in Figure 9. The increase in high-frequency energy and flattening of spectra by deconvolution is apparent in Figure 8. Figure 9 shows greater than expected attenuation in energy in frequencies higher than 45 Hz. This attenuation was not investigated in detail, although inspection of records suggested that the spectral whitening by deconvolution magnified some high-frequency incoherent energy that was suppressed by the stacking procedure.

Figure 10 shows a plot of Q-values estimated from slopes of spectra (crosses) and from spectra over successive windows (circles) for two profiles, which cross at the location of the well used in Figure 3. The Q estimates from spectra over successive windows show a smaller range than the estimates from slopes. Interestingly, for both methods estimates tend to cluster around similar values. The larger scatter in spectral slope estimates is due probably to poor signal/noise ratio at higher frequencies, which are crucial in determining the slopes of the curves.

Relationship Between Q-Factor and Dispersion

Averbukh (1969) used the absorption law

$$\alpha = a.f^n$$

where α is the absorption coefficient, f the frequency, and a and n are constants for determining the velocity dispersion of elastic waves. A large number of measurements of the absorption coefficient in a variety of lithologic environments conform to the above law when $n = 1$. In this case the model predicts that the velocity at frequency f with respect to velocity at frequency f_0 is given by (Crowe and Alhilali, 1974)

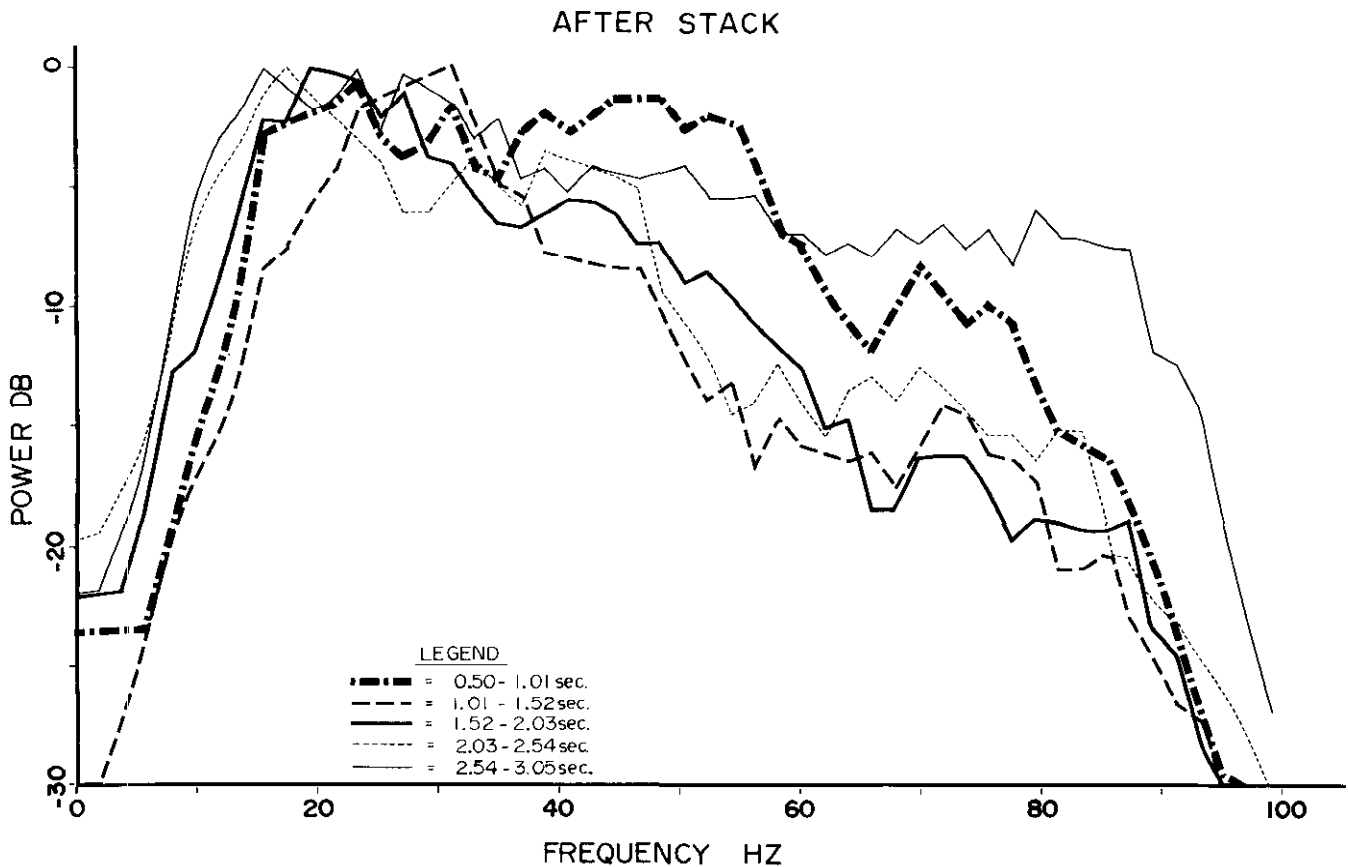


Fig. 9. Spectra over field trace after stack.

$$V(f) = V(f_0) \left[1 - \frac{\delta(f_0)}{\pi^2} \ln \frac{f}{f_0} \right]^{-1} \quad (3)$$

where δ is the logarithmic decrement defined as half of the fractional energy absorbed per cycle. Normally, a variation of δ with frequency is so small as to be negligible. By substituting $\delta = \pi/Q$, Equation (3) becomes

$$V(f) = V(f_0) \left[1 - \frac{1}{\pi Q} \ln \frac{f}{f_0} \right]^{-1} \quad (4)$$

Equation (4) is the same as that quoted by O'Brien (1961) from Kolsky (1956). If $\Delta V = V(f_0) - V(f)$, the equation can be written as:

$$\frac{\Delta V}{V(f)} = - \frac{.3183}{Q} \ln \left(\frac{f}{f_0} \right) \quad (5)$$

Figure 11 shows the variation of $\Delta V/V$ for Q ranging from 30 to 300 for frequency range $10-10^6$ Hz for $f_0 = 20,000$ Hz, which is normally the frequency of the sonic logging tool.

Since the sonic log measures V in transit time, and two-way time is obtained by adding transit times, it follows that any differences in velocity between sonic frequencies and seismic frequency must cause the same differences ΔT (only with opposite algebraic sign) in two-way time T . Therefore, one can write

$$\frac{\Delta T}{T} = \frac{T(f_0) - T(f)}{T} = \frac{.3183}{Q} \ln \left(\frac{f}{f_0} \right) \quad (6)$$

Normally $f_0 = 20,000$ Hz and $F = 30$ Hz. Then,

$$\frac{\Delta T}{T} = \frac{-2.12}{Q} \quad (7)$$

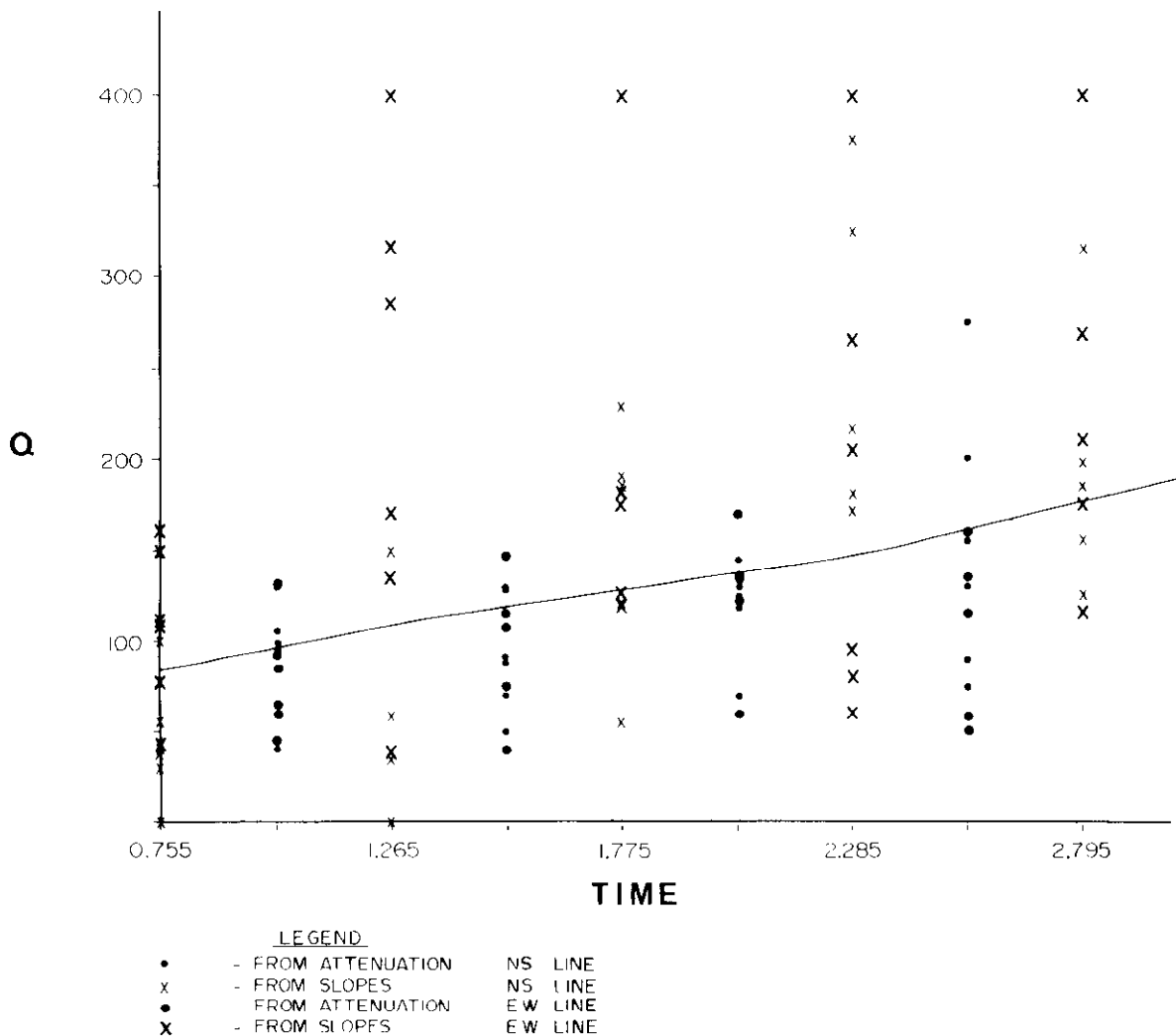


Fig. 10. Plot of estimated values of Q from slopes and windows for two seismic profiles.

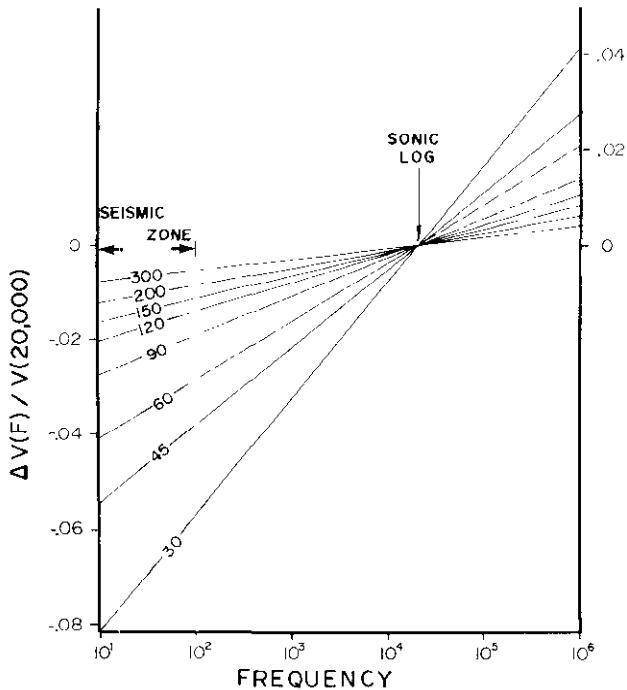


Fig. 11. Plot of change in velocity compared with velocity at 20K Hz vs Q.

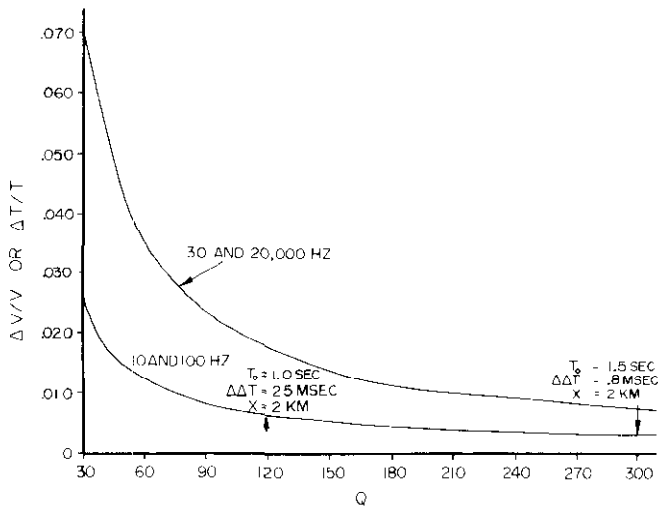


Fig. 12. Plot of change in velocity or travel time vs Q for frequencies 30 and 20,000 Hz (top) and 10 and 100 Hz (bottom).

A plot of $\Delta T/T$ vs Q is shown in Figure 12. The top curve shows the stretch one must apply on the sonic to match seismic sections for the appropriate value of Q . When $Q = 100$, the needed stretch is 21 ms over one second. When $Q = 300$, the stretch is only 7 ms.

The bottom curve in Figure 12 shows $\Delta V/V$ for frequencies of 10 and 100 Hz, two ends of the seismic spectrum. The curve is interesting for two reasons. First, it gives an indication of distortion in the wavelet for different travel times. The time difference between the 10- and 100-Hz components at 1.0 s is 6 ms for $Q = 150$ and 12 ms for $Q = 60$, which indicates that the wavelet will be broader for lower Q . Second, one can

compute, for a given spread, the difference in normal moveout corresponding to velocities at two frequencies. It was done in two cases: (a) spread 2000 m, average velocity 3000 m/s and $Q = 120$ at 1.0 s, and (b) $Q = 300$ at 1.5 s, for the same velocity and spread. The difference in velocities at the two frequencies is 0.6 and 0.25 percent, respectively. If the data were corrected for velocity appropriate for 10 Hz, overcorrection in the 100-Hz component would correspond to 2.5 ms in (a) and 0.8 ms in (b). On real data, these values are much less than errors caused by other sources like multiples, random noise, static problems, etc., and velocity dispersion caused by absorption is not likely to be significant in the stacking process.

Computation of Q From Dispersion and Correction of Sonic Logs - Examples

Equation (6) readily gives a method of computing the Q -factor from a sonic log and the seismic traces at the well. The time shift between the sonic and seismic data can be estimated by cross correlation and then substituted in Equation (6) to determine Q . The sonic can be corrected either by stretching it according to these shifts or by stretching it according to Equation (6) from computed Q -values. The latter procedure is preferred because the 'stretch' is often distorted by noise present on traces or deviation of the well, and a limited range of Q -values limits the permissible stretch.

Figure 13 shows a seismic section from central Alberta. The synthetic computed from the sonic velocities (given at the top of the figure) is shown at its proper location. The sonic needs to be stretched to find matching events between .4 and 1.4 s on the seismic data. Figure 14 shows the section compared with the synthetic after velocities were adjusted for dispersion with Q -values appropriate for the sediments (Q -values shown at the bottom of the figure). The synthetic matches the seismic data over the length of the trace and also helps to identify correct polarity. Next, a wavelet was computed from the seismic section and applied to the sonic to generate a synthetic trace, which was used to estimate Q by comparing this synthetic with the computed wavelet to the seismic section. The final synthetic, computed after correcting for Q (Fig. 15), matches the data very well for the length of the sonic, and a local zone of compaction around .8 s is indicated.

Figure 16 shows the seismic section crossing a well from offshore Africa. These data were used in computing the Q -factor in Figure 10. The match between the synthetic and the data is reasonable but, again, the synthetic needs to be stretched to match over its total length. Figures 17 and 18 show the comparisons after velocities have been adjusted for Q -values computed by comparing synthetic and stacked seismic data and Q -values computed in Figure 10, respectively. Both show a significantly improved match. In this instance, Q -values computed from field records appear to give a

CENTRAL ALBERTA

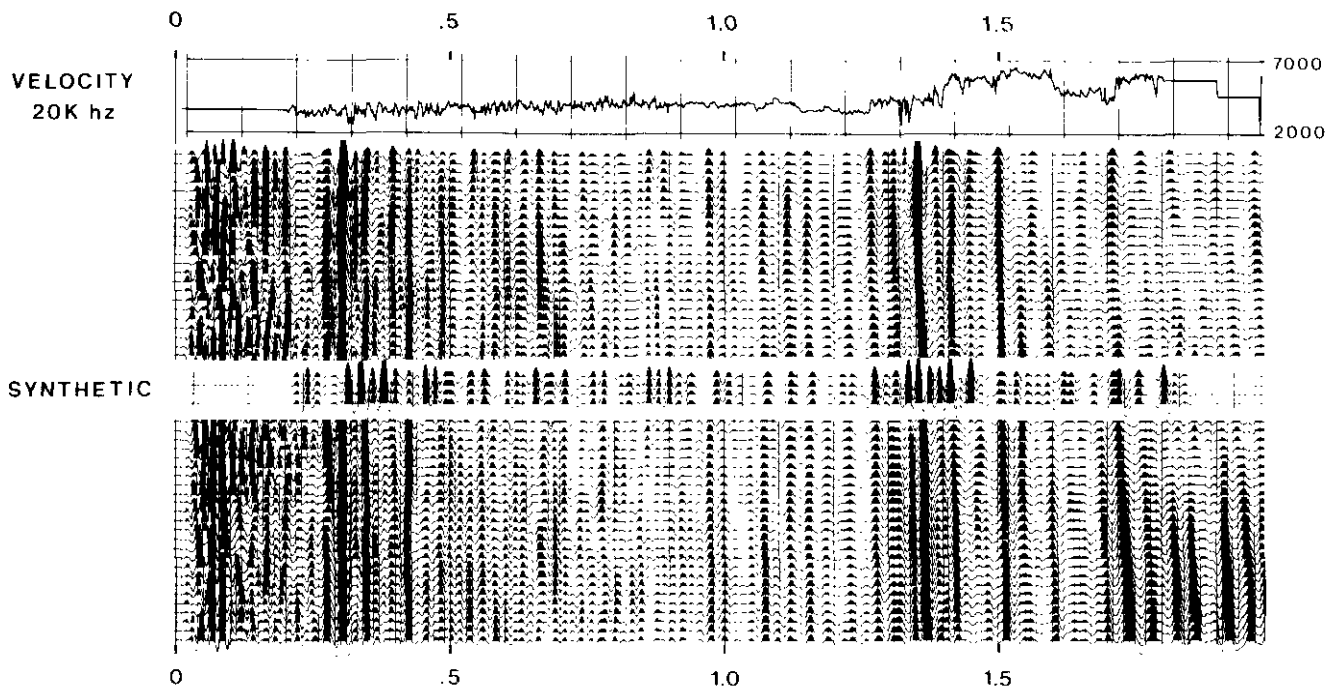


Fig. 13. Comparison of synthetic seismogram and the seismic section from central Alberta

CENTRAL ALBERTA

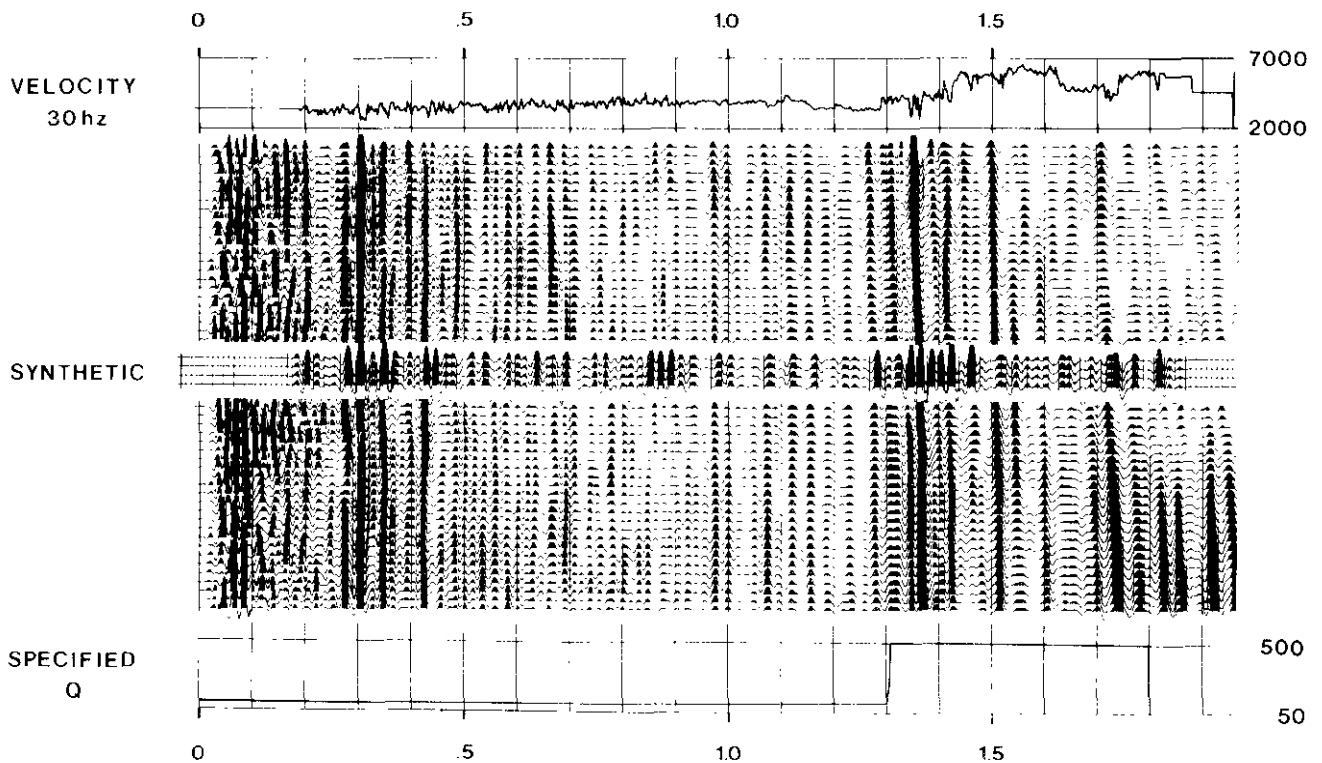


Fig. 14. Comparison of synthetic trace and synthetic seismogram after sonic is adjusted for assumed Q

CENTRAL ALBERTA

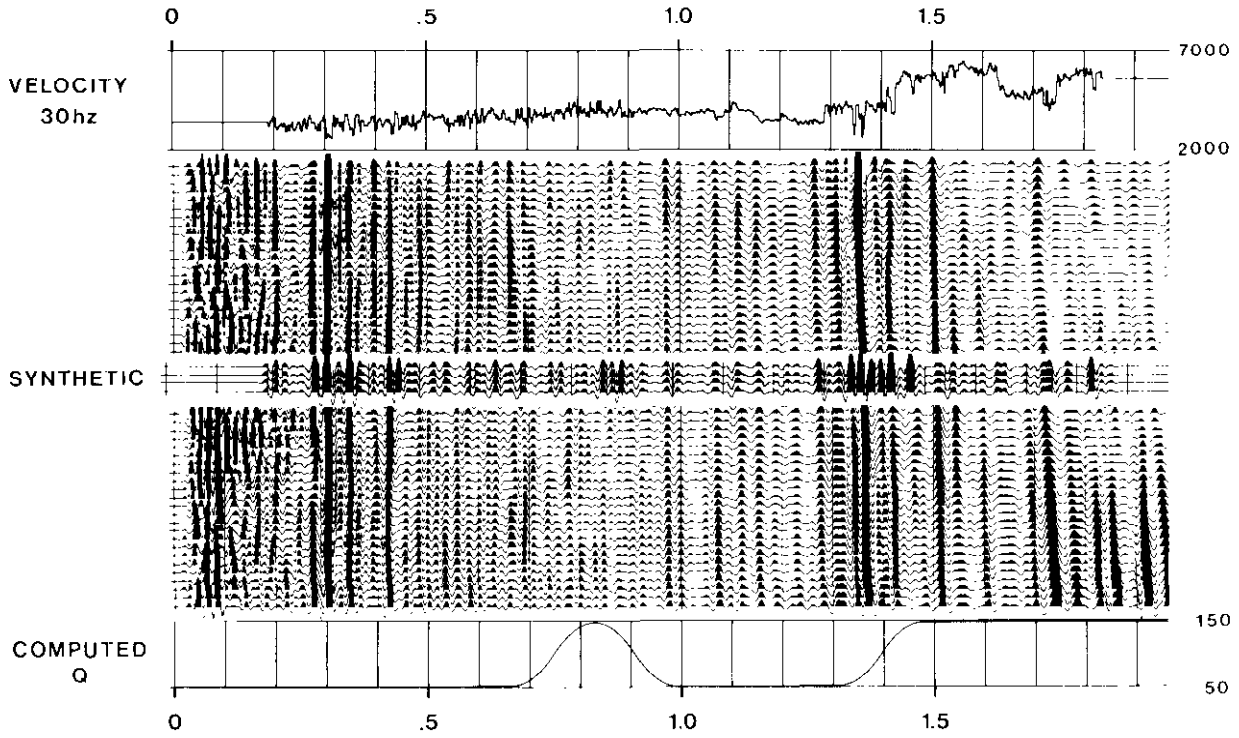


Fig. 15. Comparison of synthetic trace and synthetic seismogram after sonic is adjusted for computed values of Q.

OFFSHORE AFRICA

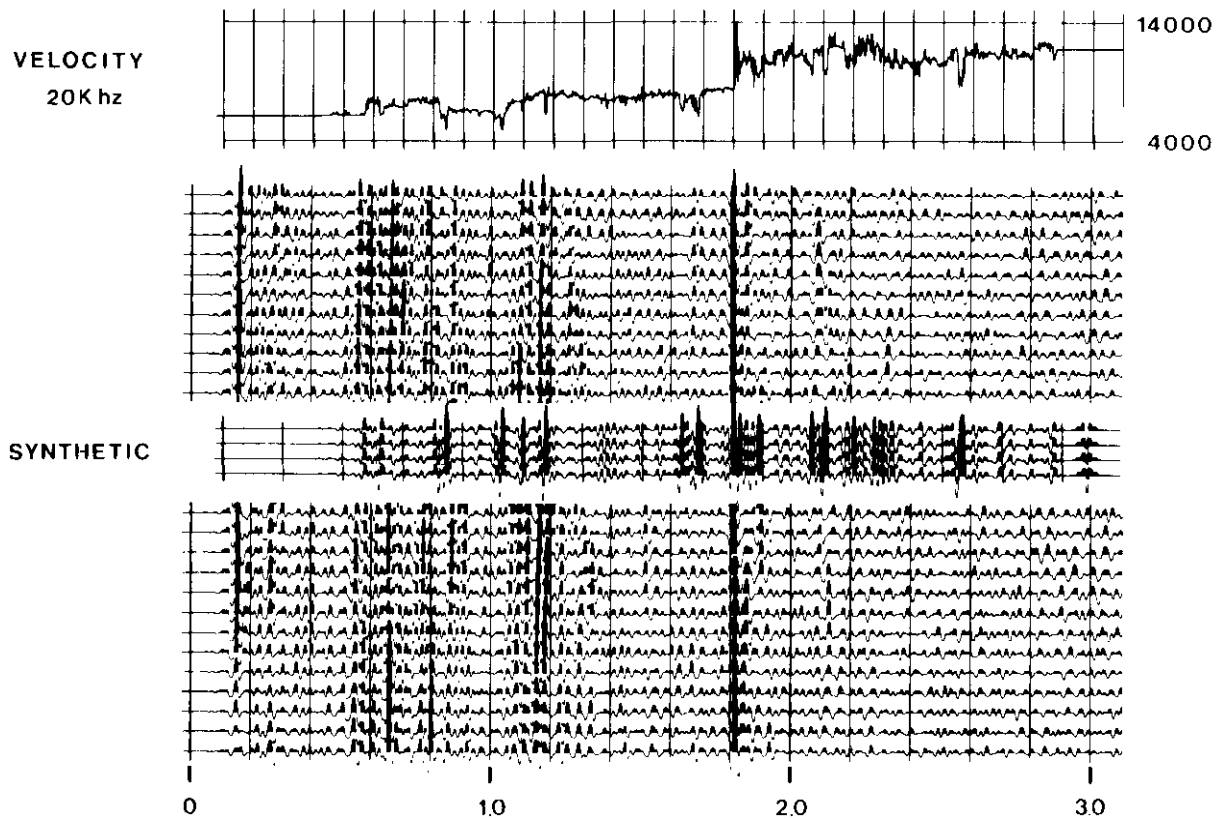


Fig. 16. Comparison of synthetic trace and seismic section from offshore Africa.

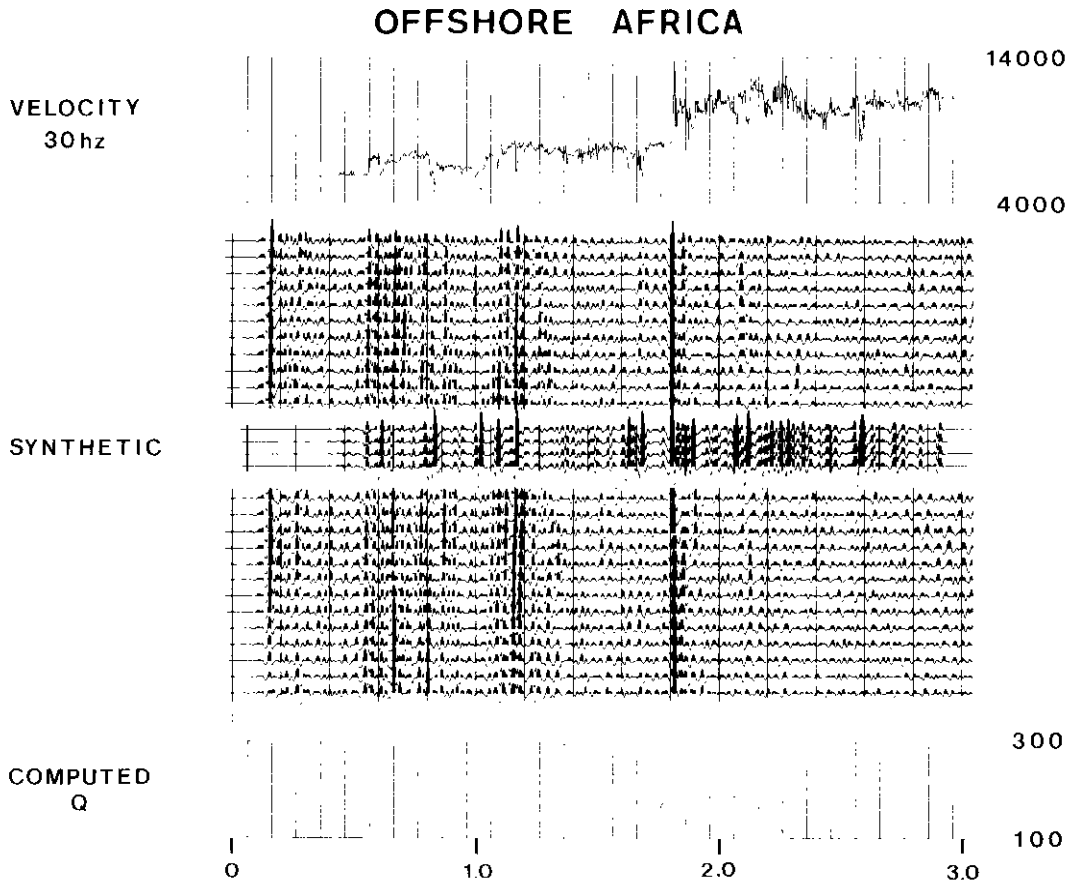


Fig. 17. Comparison of synthetic trace after adjustment of Q (computed from stretch) and seismic section.

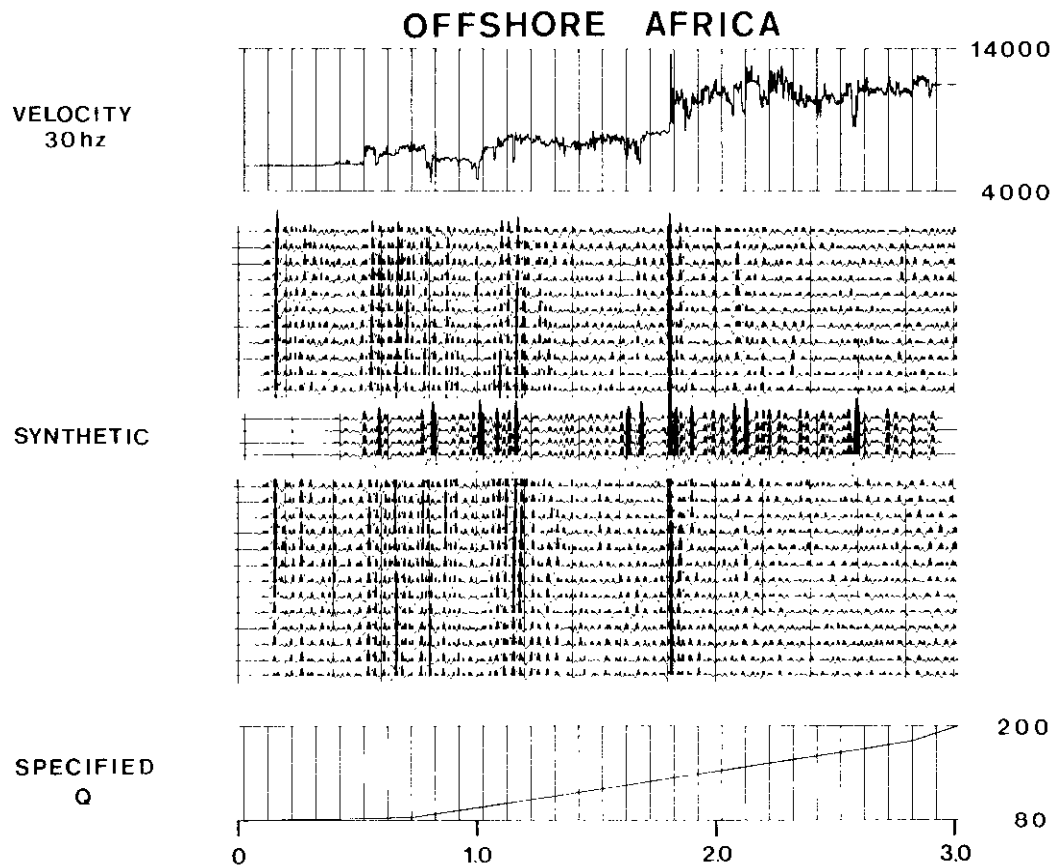


Fig. 18. Comparison of synthetic trace after adjustment of Q computed in Figure 10 and seismic section

NORTHERN ALBERTA

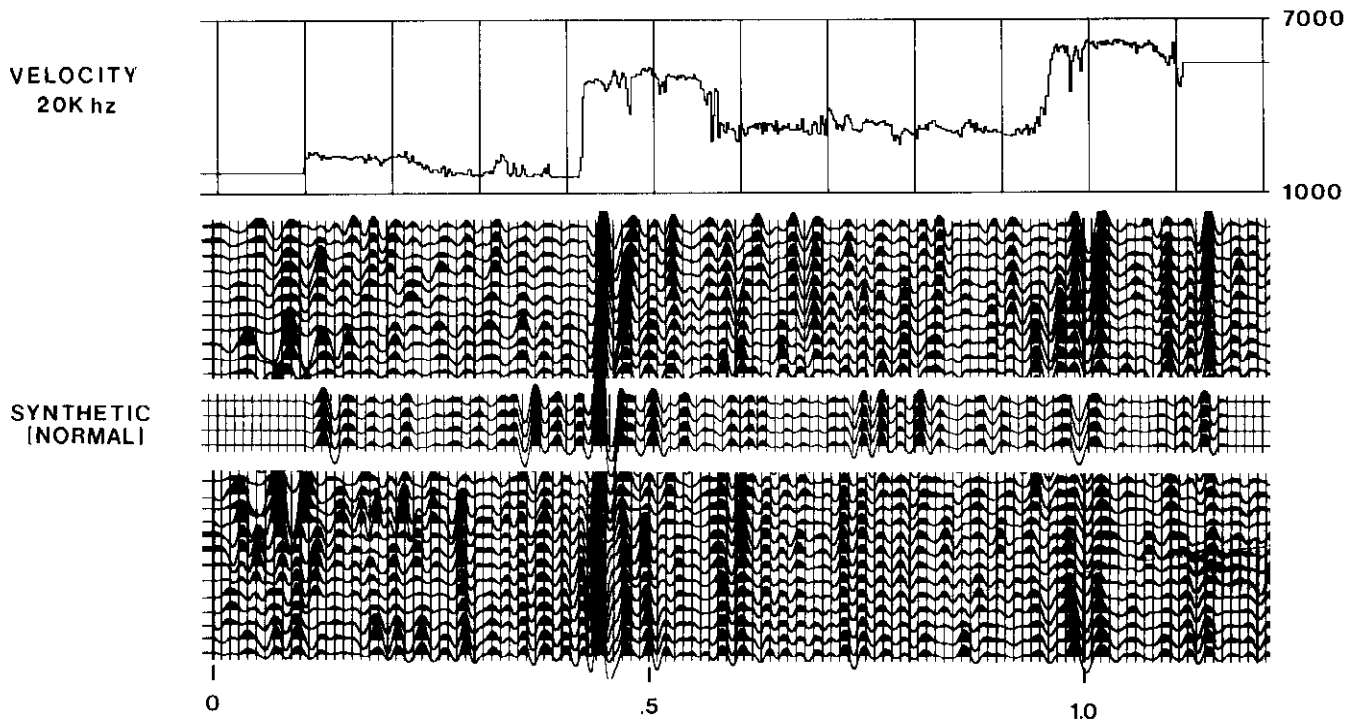


Fig. 19. Comparison of synthetic trace (normal polarity) and seismic section from northern Alberta.

NORTHERN ALBERTA

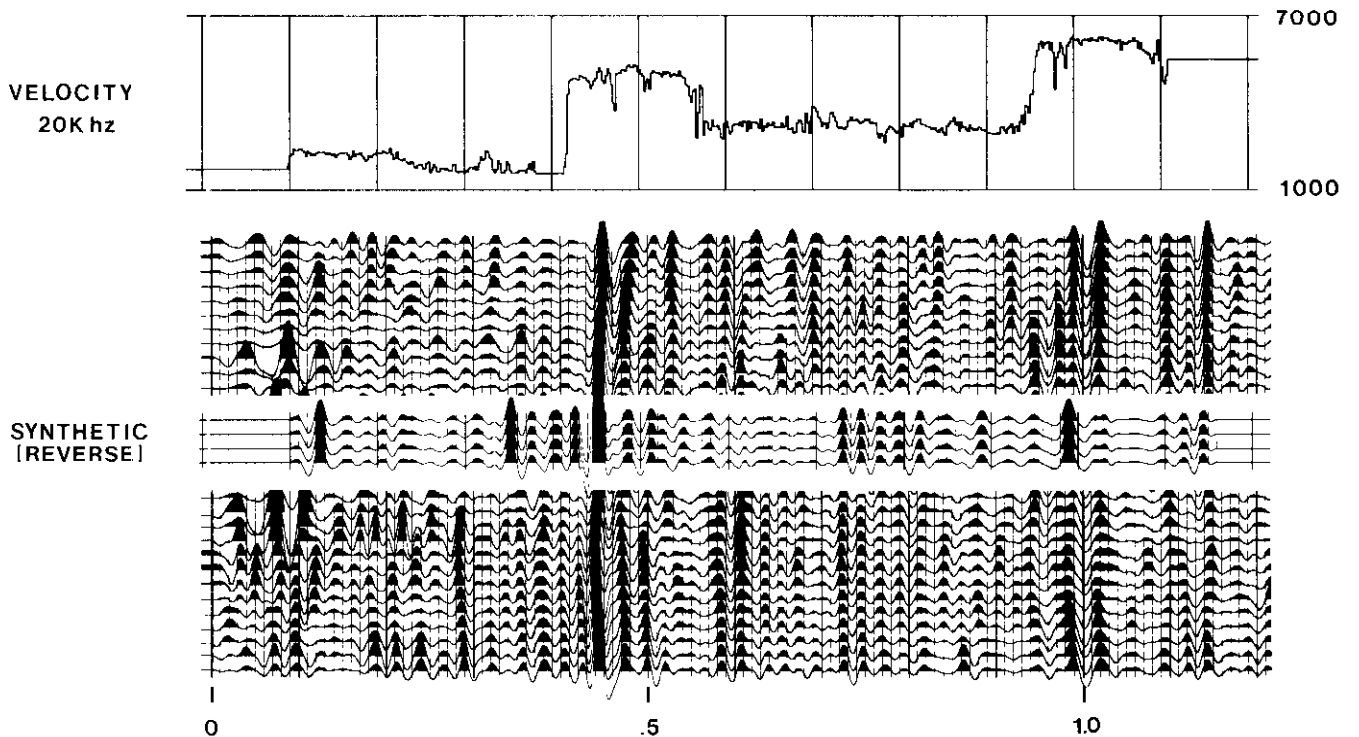


Fig. 20. Comparison of synthetic trace (reverse polarity) and seismic section from northern Alberta.

better fit. We do not yet have enough experience to say whether such is generally the case.

Figures 19 and 20 show synthetics with both polarities matched to the stacked data across the well from Sigma's north Alberta regional study. A case can be made for either polarity matching the data, allowing some stretch in the sonic in Figure 19 and being tolerant of character mistie around 1.0 s in Figure 20. The synthetic for Figure 21 is displayed with normal polarity, and was computed after velocities had been corrected for Q-values estimated from lithology. The match between this synthetic and the stacked data is reasonable for Mississippian (.43 s) and Slave Point (.98 s) markers, both in travel time and in character. This confirms that normal polarity is preferable on these data for stratigraphic studies.

Figures 22 and 23 show the example where seismic velocities were changed to sonic frequencies. Figure 22 shows a central Alberta inverted section with the sonic

velocities overlaid at the correct location. It is a good match but, again, the sonic needs some stretch. Figure 23 shows the match after inverted velocities and travel times were adjusted for dispersion. The match with the overlaid sonic is excellent, and changes in the sonic can be correlated directly to an event on the inverted section.

CONCLUSION

It has been shown that the Q-absorption is crucial in determining the attainable limits of seismic resolution, and that this factor can explain the mistie between seismic-sonic times. Q-values can be computed either from the seismic field records or from a comparison of stack sections with synthetic seismograms. Synthetic studies show that Wiener-Levinson deconvolution corrects for distortion and delays in the wavelet caused by absorption within the seismic spectrum.

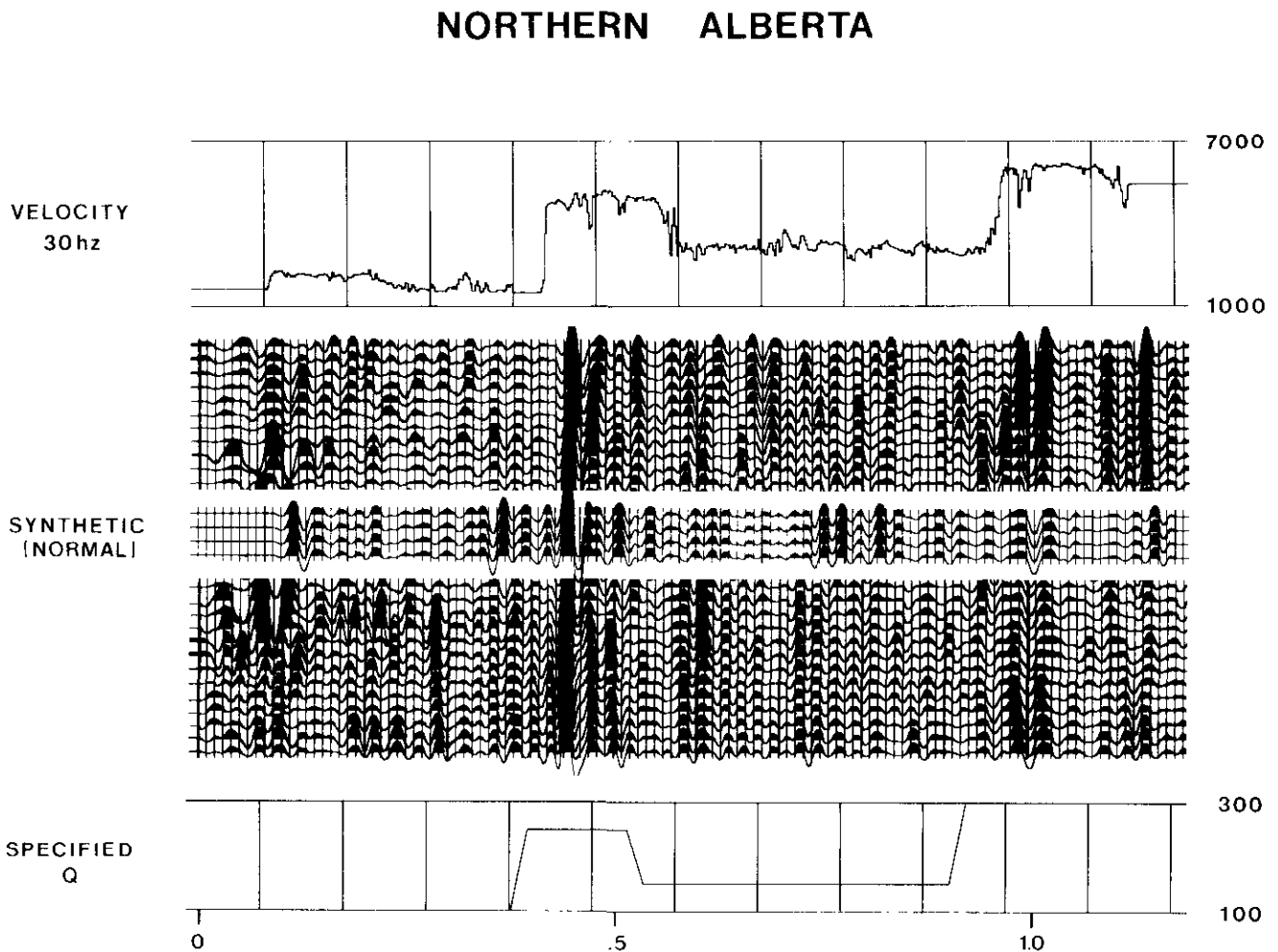


Fig. 21. Comparison of synthetic trace after Q correction (normal polarity) and seismic section from northern Alberta.

CENTRAL ALBERTA

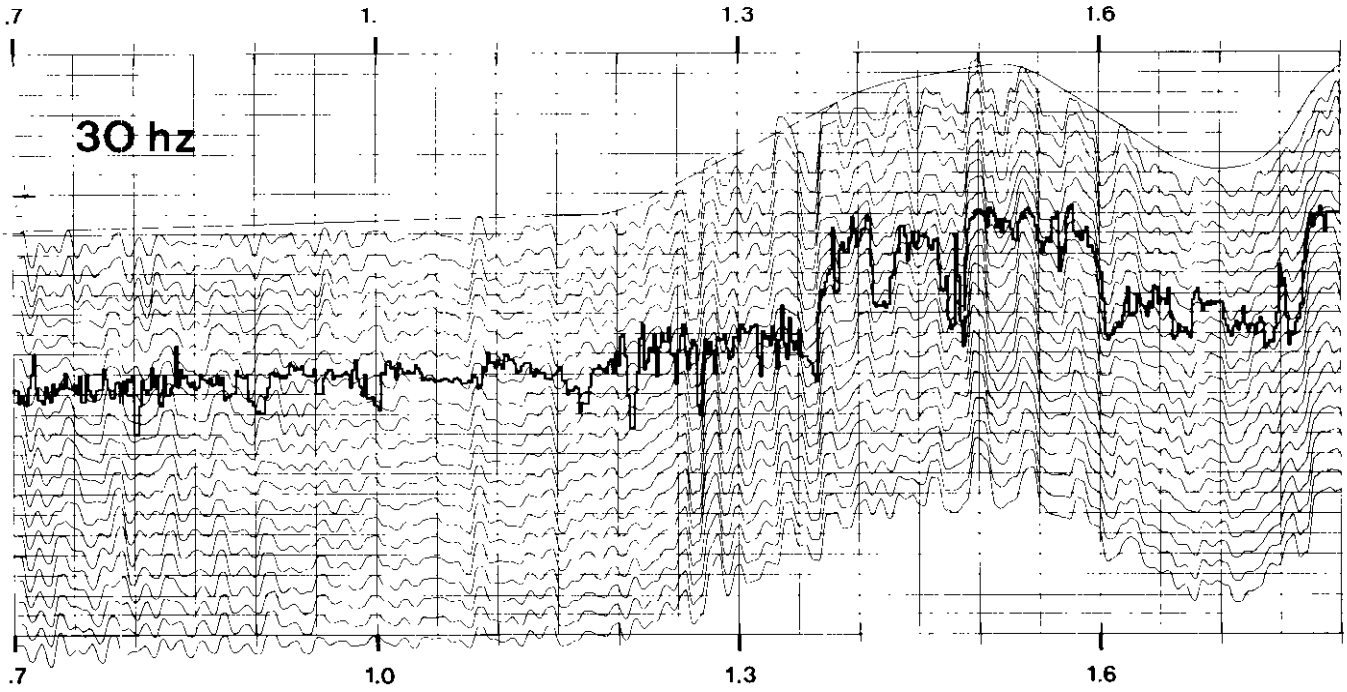


Fig. 22. Comparison of inversion section with sonic, central Alberta.

CENTRAL ALBERTA

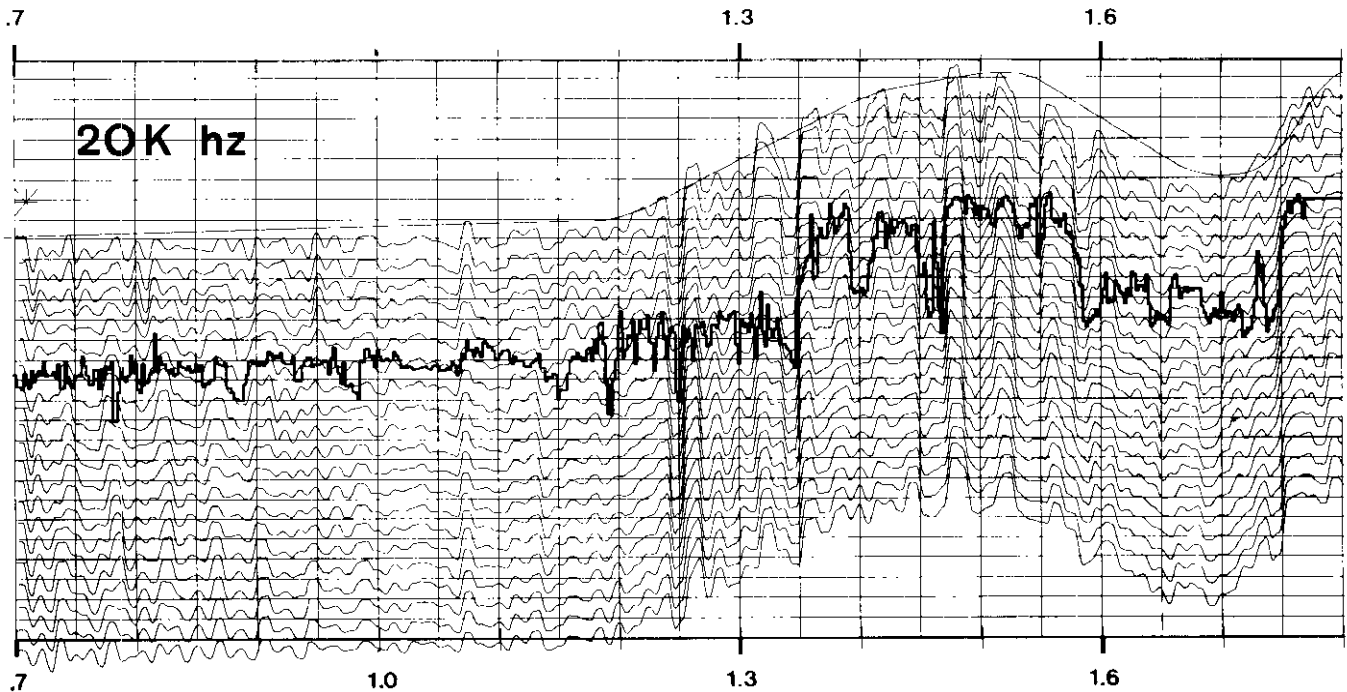


Fig. 23. Comparison of inversion section after adjustment of expected Q with sonic, central Alberta.

REFERENCES

- Averbukh, A.G., 1969, The determination of velocity dispersion of elastic waves from amplitude characteristics of a medium: *Prikladnaya Geofizika (Applied Geophysics)*, No. 57, p. 50-60.
- Bremaecker, J.C.L., Godson, R.H., and Watkins, J.S., 1966, Attenuation measurements in the field: *Geophysics*, v. 31, p. 562-569.
- Crowe, C. and Alhilali, K., 1975, Attenuation of seismic reflections as a key to lithology and pore filler: 60th Annual Meeting of AAPG, Dallas, Texas.
- Futterman, W.L., 1967, Dispersive body waves: *Journal of Geophysical Research*, v. 67, p. 5279-5291.
- Ganley, D.C. and Kanasewich, E.R., 1980, Measurements of attenuation and dispersion from check shot surveys. *Journal of Geophysical Research*, v. 85, p. 219-226.
- Gardner, G.H.F., Wyllie, M.R.J. and Droschak, D.M., 1964, Effects of pressure and fluid saturation on the attenuation of elastic waves in sands: *Journal of Petroleum Technology*, v. 16, p. 189-198.
- Gretener, P.E.F., 1961, An analysis of the observed time discrepancies between continuous and conventional well velocity surveys: *Geophysics*, v. 26, p. 1-11.
- Knopoff, L. and MacDonald, G.J.F., 1958, Attenuation of small amplitude stress waves in solids: *Reviews of Modern Physics*, v. 30, p. 1178-1192.
- Kolsky, H., 1956, The propagation of stress pulses in viscoelastic solids: *Philosophy Magazine, Series I*, v. 8, p. 693-710.
- McCarley, L.A., 1985, An autoregressive filter model for constant Q attenuation: *Geophysics*, v. 50, p. 749-758.
- McDonal, F.J., Angona, F.A., Mills, R.L., Sengbush, R.L., Van-
Nostrand, R.G. and White, J.C., 1958, Attenuation of shear and compressional waves in Pierre shale: *Geophysics*, v. 23, p. 421-439.
- O'Brien, P.N.S., 1961, A discussion on the nature and magnitude of elastic absorption of seismic prospecting: *Geophysical Prospecting*, v. 9, p. 261-275.
- Stewart, R.R., Huddleston, P.D. and Tze, K.K., 1984, Seismic versus sonic velocities: a vertical seismic profile study: *Geophysics*, v. 49, p. 1153-1168.
- Strick, E., 1967, The determination of a dynamic viscosity, and transient creep curves from wave propagation measurements: *Geophysical Journal of the Royal Astronomical Society*, v. 13, p. 197-218.
- —, 1970, A predicted pedestal effect for pulse propagation in constant Q solids: *Geophysics*, v. 35, p. 387-403.
- —, 1971, An explanation of observed time discrepancies between continuous and conventional well velocity surveys: *Geophysics*, v. 36, p. 285-295.
- Trorey, A.W., 1962, Theoretical seismograms with frequency and depth dependent absorption: *Geophysics*, v. 27, p. 761-785.
- Winkler, K.W., 1986, Estimates of velocity dispersion between seismic and ultrasonic frequencies: *Geophysics*, v. 51, p. 183-189.
- Wuenchel, P.C., Dispersive body waves — an experimental study: *Geophysics*, v. 30, p. 539-551.